

# Chapter 23

## Effect of Welding Processes on the Mechanical Properties of Hardox 400 Steel Welded Joints



Ranbir Singh Multani, Varun Sharma, Ajay Gupta, and Jaswant Singh

**Abstract** The present paper investigates the effect of gas metal arc welding process and shielded metal arc welding process on the tensile, impact, and metallurgical properties of 20 mm quenched and tempered steel welded joints. To accomplish the established aim, double V groove joints with 60° groove angle were welded using gas metal arc welding process and shielded metal arc welding process using low hydrogen ferritic steel consumables. Microhardness studies carried out along and across the welded joints accompanied by the microstructural investigations revealed significant variation within the fusion and the heat affected zone of the weldments. Tensile and impact property studies of the shielded metal arc welding process welded joint shown better properties as compared to the gas metal arc welding process owing to the presence of fine acicular ferrite in the fusion zone due to low heat input. Extensive tempering due to weld thermal cycles has shown a more detrimental effect on the hardness of heat affected zone of all the welded joints with the reduction in hardness to around 50–60% for approximately 70 mm width around welded region.

**Keywords** Hardox 400 · Shielded metal arc welding process · Gas metal arc welding process · Microhardness · Microstructure · Mechanical properties

---

R. S. Multani (✉) · V. Sharma · A. Gupta  
Department of Industrial & Production Engineering, Dr B R Ambedkar National  
Institute of Technology, Jalandhar 144011, India  
e-mail: [ranbirking18@gmail.com](mailto:ranbirking18@gmail.com)

V. Sharma  
e-mail: [sharmav@nitj.ac.in](mailto:sharmav@nitj.ac.in)

A. Gupta  
e-mail: [guptaa@nitj.ac.in](mailto:guptaa@nitj.ac.in)

J. Singh  
Department of Mechanical Engineering, Dr B R Ambedkar National Institute of Technology,  
Jalandhar 144011, India  
e-mail: [jaswantsingh@nitj.ac.in](mailto:jaswantsingh@nitj.ac.in)

## Nomenclature

GMAW	Gas metal arc welding
GTAW	Gas tungsten arc welding
UTS	Ultimate tensile strength
BHN	Brinell hardness number
VHN	Vicker's hardness number
ASTM	American Society for Testing and Materials
JG	Joint welded using GMAW process
JS	Joint welded using SMAW process
WCL	Weld center line
SCHAZ	Sub-critical heat affected zone
ACF	Acicular ferrite
PF	Polygonal ferrite

### 23.1 Introduction

Low-alloy steels having the total alloying content less than 5% and those in the quenched and tempered conditions possess high yield strength of 560 N/mm<sup>2</sup> to 880 N/mm<sup>2</sup>, greater notch toughness and nominal hardness. A sharp increase in wear resistance (by factors of 3–5) is seen only when tensile strength is increased to 1050–1400 MPa [1]. Currently, a new-generation modern steels are being used in the extreme engineering applications which possess very high tensile strength of UTS > 1200 MPa and high hardness around 400–600 BHN [2]. These steels find applications in the areas requiring high resistance to abrasion in chutes, hoppers, dump truck beds, cutter bars, scraper blades, liner plates, tipper bodies, containers, crushing mills, mills, excavator buckets and loading buckets, etc. [3–5].

Hardox 400 is one such standard type abrasion resistant steel developed which shows high hardness of around 400 BHN and high tensile strength of 1250 MPa, good weldability with certain precautions and good machinability. Currently, this steel is being used frequently in buckets and liner plates. GMAW, GTAW, SMAW, and FCAW are the commonly used processes used to weld this category of steels [6–8]. Generally, undermatched welds are used in joining these high strength steels with the aim of minimizing the hydrogen-induced cracking tendency [9, 10]. Apart from this, the commonly observed phenomenon that takes place in the welding of these steels is reduction in the hardness and strength of HAZ, improvement in the toughness of the weld zone but overall reduction in hardness and tensile strength of weld, etc., due to the weld heat thermal cycles, use of low heat input welding processes, and use of filler materials of low strength [11]. This paper reports the influence of GMAW and SMAW processes on the mechanical properties of welded joints fabricated by keeping minimum heat input. Ballistic performance of the armor grade steel welded joints, possessing unequal and equal double V joint configurations, and welded with

austenitic stainless steel using SMAW process, revealed that, the unequal double V joint configuration offered maximum resistance to the penetration of the bullet at the weld metal position and without any bulge at the rear position [12]. Similar investigations related to joint design variations of quenched and tempered steels using double V, double U, and mixed joint designs welded with ferritic filler materials using SMAW process have been studied in the literature [13].

## 23.2 Experimentation

The base metal used in this study was 20 mm thick quenched and tempered steel of grade name Hardox 400. Two welded joints were produced in the coupon plates of size 250 × 125 × 20 mm using gas metal arc welding (GMAW) and shielded metal arc welding (SMAW) process. The chemical composition of the base metal and filler materials in the as received conditions is presented in Table 23.1. The mechanical properties of the base metal and the filler material in the as received condition are given in Table 23.2.

Double V groove joint with 60° groove angle and 2 mm root face was used in this study for preparing welded joints as shown in Fig. 23.1a. The test coupons were cleaned and clamped with C-clamps onto a fixture that was provided with a recess to lay down the other side weld. Before welding, the plates were preheated to a temperature of 100 °C as shown in Fig. 23.1b. One of the welded joints named JG was prepared using 2.15 mm diameter ER70s electrode using GMAW process with a mixture of argon and CO<sub>2</sub> as shielding gas. The joint named JS was prepared using 3.15 mm diameter electrode using SMAW process.

The welding parameters used during welding of both types of joints and the heat input used for laying each pass are given in Table 23.3. The heat calculating was done as per Eq. 23.1.

$$\text{Heat Input} = \eta \frac{VI}{S}$$

$$\eta = \text{arc efficiency, } V = \text{Voltage (V), } I = \text{Current (A),}$$

$$S = \text{Speed (mm/s)} \quad (23.1)$$

The arc efficiency for SMAW process and GMAW process was taken as 80% and 90%, respectively [14].

The specimens for mechanical and metallurgical testing were extracted as per the schematic shown in Fig. 23.2. Specimens used in the characterization of the microstructure, hardness, toughness, and tensile properties were extracted in a direction transverse to the welds. The macrostructures were analyzed through stereo zoom microscope. The microstructures of the joints were analyzed at various locations using optical microscope. The specimens were etched in 2% nital to reveal the

**Table 23.1** Chemical composition of base metal and filler materials in wt%

Material	Chemical composition (wt%)										
	C	Si	Mn	P	S	Cr	Ni	Mo	B		
Hardox 400	0.13	0.49	1.42	0.007	0.001	0.04	0.005	0.012	0.002		
E7018	0.15	0.75	1.6	0.035	0.035	0.2	0.3	–	–		
ER70S-6	0.07	0.67	1.22	0.009	0.013	–	–	–	–		

**Table 23.2** Mechanical properties of base metal and filler material

Mechanical properties of base material					
Material	Tensile strength (MPa)	Yield strength (MPa)	Impact energy (J)	Hardness (HV)	Elongation (%)
Hardox 400	1250	800–1100	60	340–400	10
Mechanical properties of filler materials					
AWS code	Process	Electrode diameter	Manufacturer	Yield strength (MPa)	Tensile strength (MPa)
E 7018	SMAW	3.15 mm	Ador	470	555
ER 70s-6	GMAW	2.15 mm	Ador	450	560

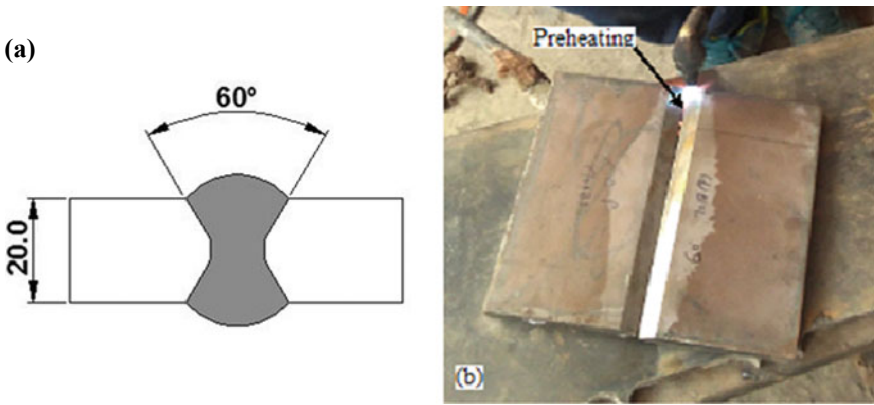


**Fig. 23.1** a Double V groove design, b base metal plate after machining and illustrating preheating

microstructure of the weldments at the weld metal, fusion zone, and HAZ. The hardness measurements were carried out as per ASTM E-384-05 standard [15] using Vickers microhardness testing machine along weld center line (WCL) and across the WCL with 1000 gm load for a dwell time of 20 S.

The tensile test specimens as illustrated in Fig. 23.3a–c were extracted and prepared according to ASTM E-8 standard [16]. These tests were conducted at room temperature on a 60 ton static universal testing machine to obtain UTS, yield strength, percentage elongation, etc. Charpy impact toughness test specimens were extracted and prepared according to ASTM E-23 standard [17] and tested on a 300 J impact testing machine as shown in Fig. 23.3d.

**Table 23.3** Welding process parameters and heat input of welded joints

Pass no.	Current (I)	Voltage (V)	Length (mm)	Time (s)	Speed (mm/min)	Efficiency	Heat input (KJ/mm)	Average (kJ/mm)
<i>Joint JS E 7018 (SMAW)</i>								
1	132	30	250	81	185.18	0.8	1.03	1.119
2	132	30	250	88	185.18	0.8	1.115	
3	132	30	250	84	185.18	0.8	1.06	
4	132	25.5	250	79	588.23	0.8	0.85	
5	133	25.5	250	89	588.23	0.8	0.965	
6	133	25.5	250	86	588.23	0.8	0.933	
7	133	25.5	250	110	588.23	0.8	1.19	
8	133	25.5	250	159	588.23	0.8	1.756	
<i>Joint JG ER 70S-6 (GMAW)</i>								
1	250	32	250	79	3.16	0.9	2.27	2.20
2	250	32	250	81	3.09	0.9	2.3	
3	250	32	250	78	3.27	0.9	2.20	
4	250	32	250	80	3.15	0.9	2.28	
5	250	32	250	77	3.4	0.9	2.1	
6	250	32	250	78	3.3	0.9	2.18	
7	250	32	250	76	3.5	0.9	2.05	
8	250	32	250	80	3.17	0.9	2.27	

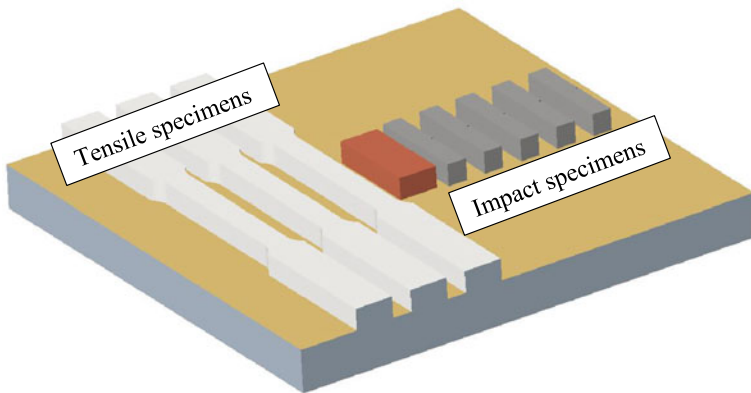


**Fig. 23.2** Mechanical and metallurgical specimens extraction schematic

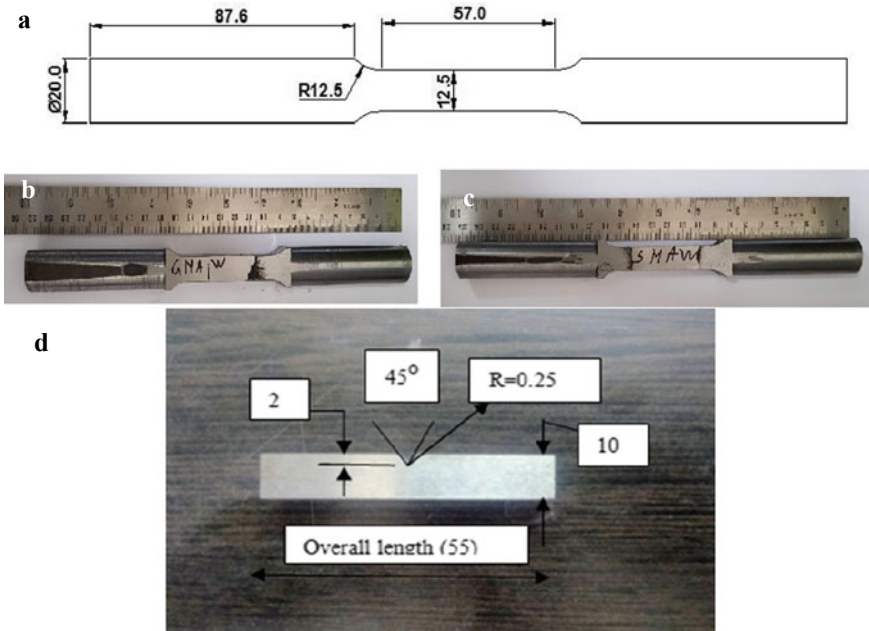


**Fig. 23.3** a Schematic of tensile specimen, b tensile specimen of JG welded joint, c tensile specimen of JS welded joint, and d impact specimen with specifications

### 23.3 Results and Discussion

#### 23.3.1 Microstructure

The microphotographs of the base metal and the welded joints were captured under different magnifications to carry out their microstructural investigations.

The micrograph of base metal shown in Fig. 23.4a clearly indicates the extra fine microstructure of acicular tempered martensite consisting of lath martensite which is separated by high angle boundaries. Similar microstructure of Hardox 400 had also been observed in the literature which is responsible for enhancing yield strength, hardness, and toughness of the steels [15]. The micrographs taken at the fusion zone of JG and JS welded joints indicate the presence of acicular ferrite (ACF) within the grain surrounded by polygonal ferrite (PF) content at the grain boundaries as shown in Fig. 23.4b. However, the presence of larger amount of PF (white region) in JG joint as shown in Fig. 23.4c indicates higher heat input in GMAW process as compared to JS joint with lower heat content by the SMAW process. Significant tempering of base metal in the sub-critical region of heat affected zone (HAZ) led to the coarsening of tempered martensite which is clearly evident from Fig. 23.4d.

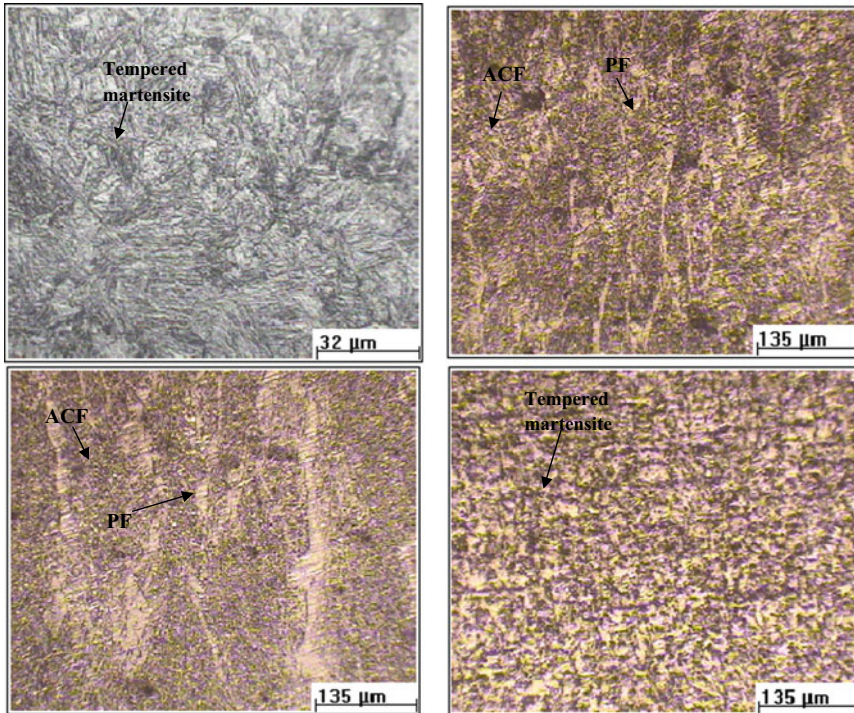


**Fig. 23.4** Micrographs: **a** base metal, **b** welded joint JG, **c** welded joint JS and **d** sub-critical region of heat affected zone

### 23.3.2 Hardness

The hardness measurements were carried out in two different directions to evaluate the hardness variations both along and across the weld cross section. The microhardness values along weld center line are shown by *Y-Y* axis and across the weld cross section are represented by *X-X* axis. Microhardness plots along and across weld center line (WCL) are shown in Fig. 23.5 for JG and JS welded joints.

As observed from the plot for hardness variation along WCL, the average hardness of weld zone for JS joint was found to higher than the JG joint. It is further observed that for both the joints, the plot shows an increase in hardness at the root pass, which could be attributed to the higher dilution of base metal toward the root pass region. Microhardness plot across WCL for both the welded joints shows almost same hardness values at the weld zone. However, hardness dips to minimum value of 180.1 and 182.9 VHN for JS and JG joints, respectively, signifying the sub-critical heat affected zone (SCHAZ) which could have been developed due to excessive tempering effect. Further, traverse across WCL shows consistent increase in microhardness values owing to the decreasing tempering effect on the base metal. This could further be revealed from the microhardness plots that even after approaching 12 mm distance



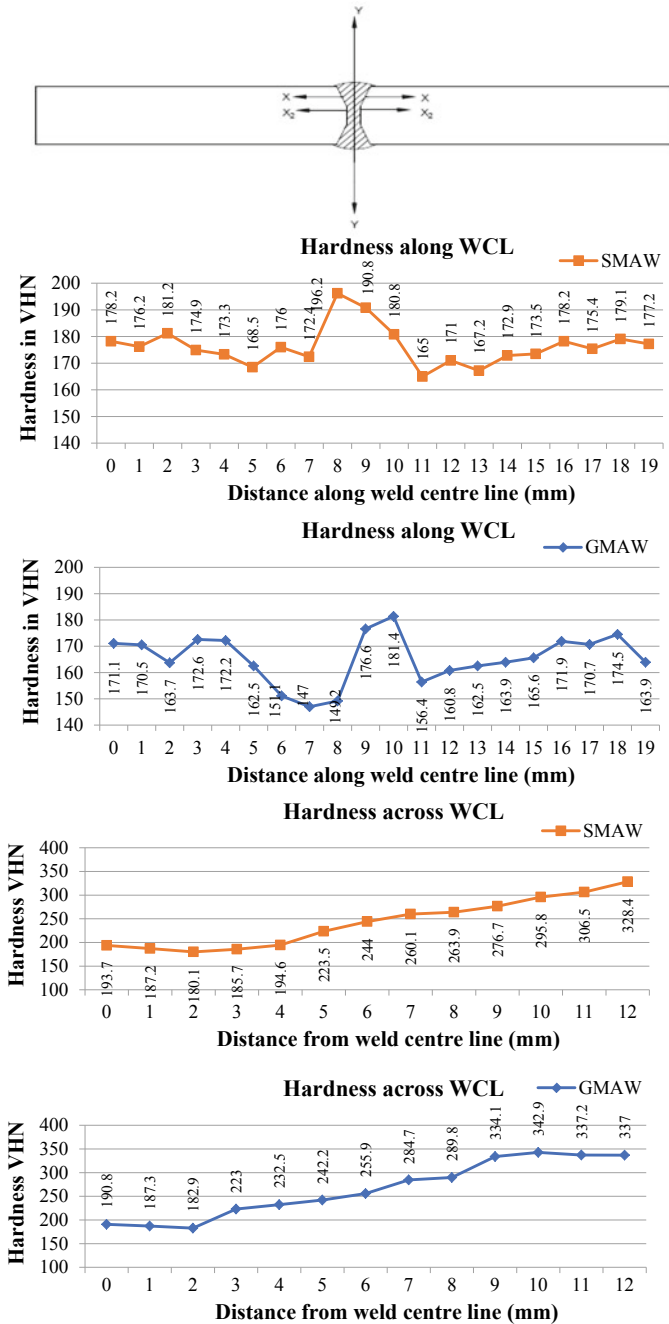


Fig. 23.5 Graphical representation of microhardness along and across weld center line (WCL) for the welded joints welded using SMAW and GMAW process

**Table 23.4** Tensile properties of base metal and welded joints

Joint type	Tensile properties					
	Yield strength (Mpa)	Ultimate tensile strength (Mpa)	(%)	Strength ratio (YS/UTS)	Joint efficiency (%)	Failure zone
Hardox 400	1000	1250	10.00	0.80	–	Base metal
JG	528	580	13.18	0.91	52.8	Weld metal
JS	560	600	20.51	0.93	56.0	Weld metal

from the weld center line for JS and JG welded joints, the microhardness reached up to 328 VHN and 337 VHN, respectively, indicating the large HAZ present in the quenched and tempered steels.

### 23.3.3 Tensile Properties

Transverse tensile properties of the base metal and the welded joints evaluated in accordance to ASTM E8 standard are given in Table 23.4.

During the tensile test, all the specimens (both types of joints) were found to fracture in the weld metal region indicating the weld zone to be the weakest link within the weldment. The JS joint shows higher UTS of 600 MPa, thus resulting in joint efficiency of 56% as compared to UTS of 580 MPa with joint efficiency of 52.8% for the JG joint. Further, it could be observed from the table that the JS joint shows higher ductility with 20.51 percentage elongation as compared to 13.18% for the JG joint which could be attributed to the higher heat input in the JG joint as compared to the JS welded joint. The higher ductility of the JS joint can further be visualized from the fractured ends of tensile sample shown in Fig. 23.6a, b which predicts an appreciable level of ductility possessed by the welded joint. The better ductility as possessed by the JS welded joint is also evident from Fig. 23.6b, d, where a higher degree of necking and protruded shear lips are observed as compared to the JG welded joint (Fig. 23.6a, c).

Its good ductile behavior can be further assessed from the shear lips and the extrusion at the center of fractured end as shown in Fig. 23.6c, d.

### 23.3.4 Toughness

Charpy V impact tests for the JG and JS welded specimens were carried out at room temperature to determine their impact toughness. The results show that the JS welded joint possessed impact toughness of 194 J as compared to JG joint (170 J).

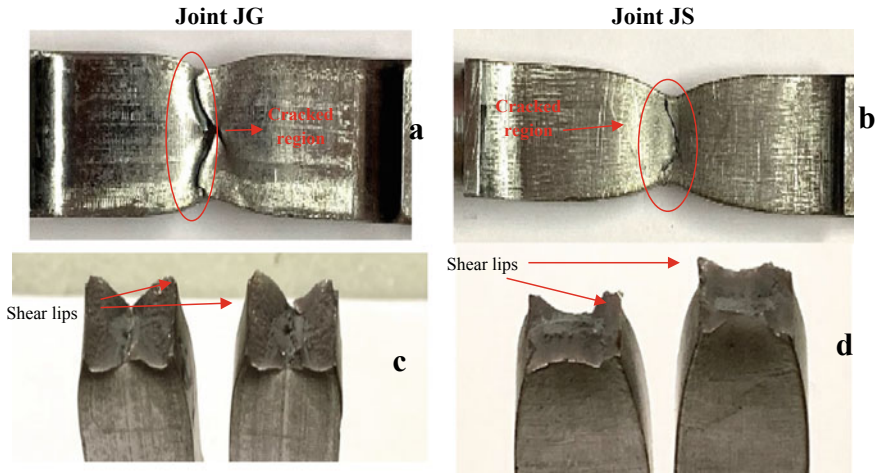


**Fig. 23.6** Optical fractographs of fractured tensile specimens of the welded joints

The outcomes from the impact tests were further analyzed by carrying out fracture analysis of impact test specimens. It can be predicted from Fig. 23.7 that after impact test, the fractured ends remained un-separated indicating high toughness and ductility of the JG and JS joints. Further, the larger shear lips area and smaller uncontrolled fractured region indicate high ductility possessed by the JS joint as compared to JG welded joint. This could be attributed to the presence of softer microstructural phases present in the JS welded joint.

## 23.4 Conclusions

Based on the current investigation, the following major conclusions are drawn:

- Owing to higher heat input in JG joint, the average hardness within the fusion zone is lower as compared to JS welded joint.
- JS joint fabricated from SMAW process shows better tensile strength and ductility as compared to JG welded joint when fabricated using similar welding electrodes.
- JS welded joint showed better Charpy V notch impact toughness as compared to JG welded joint under similar testing conditions.

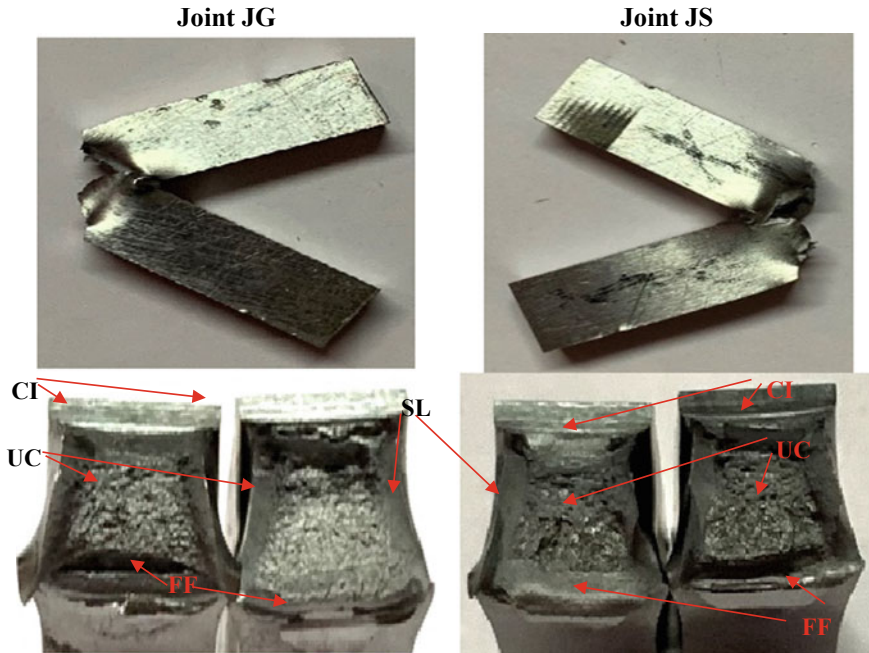


**Fig. 23.7** Optical fractographs of fractured Charpy V notch impact specimens of the welded joints; CI—Crack initiation, SL—Shear lips, FF—Final fracture, and UC—Unstable crack region

## References

- Balakrishnan, M., Balasubramanian, V., Madhusuhan, G., Sivakumar, K.: Effect of buttering and hardfacing on ballistic performance of shielded metal arc welded armour steel joints. *Mater. Des.* **32**, 469–479 (2011)
- Wang, J., Li, Y., L, P.: Effect of weld heat input on toughness and structure of HAZ of a new super high strength steel. *Bull. Mater. Sci.* **26**(3), 301–305 (2003)
- Parmar, R. S.: *Welding Engineering and Technology*. Khanna Publishers (2003)
- Manual JFE Everhard: JFE-EH series: abrasion-resistant steel plate (2004)
- Sharma, V., Shahi, S.: Quenched and tempered steel welded with micro-alloyed based ferritic fillers. *J. Mater. Process. Techn.* **253**, 2–16 (2018)
- Lakshminarayanan, A.K., Shanmugam, K., Balasubramanian, V.: Effect of welding processes on tensile and impact properties, hardness and microstructure of AISI 409 M ferritic stainless joints fabricated by duplex stainless steel filler metal. *J. Iron. Steel Res. Int.* **16**(5), 66–72 (2009)
- Ragu Nathan, S., Balasubramanian, V., Malarvizhi, S., Rao, A.G.: Effect of welding processes on mechanical and microstructural characteristics of high strength low alloy naval grade steel joints. *Defence Techn.* **11**(3), 308–317 (2015)
- Yayla, P., Kaluc, E., Ural, K.: Effects of welding processes on the mechanical properties of HY 80 steel weldments. *Mater. Des.* **28**(6), 1898–1906 (2007)
- Loureiro Altino, J.R.: Effect of heat input on plastic deformation of undermatched welds. *J. Mater. Process. Technol.* **128**, 240–249 (2002)
- Pekalski, G.: Structure and hardness changes in welded joints of Hardox steels. *Arch Civil Mech. Eng.* **VIII 4**, 15–27 (2008)

11. Sharma, V., Shahi, A.S.: Quenched and tempered steel welded with micro-alloyed based ferritic filers. *J. Mater. Process. Technol.* **253**, 2–16 (2018)
12. Balakrishnan, M., Balasubramanian, V., Reddy, G.M.: Microstructural analysis of ballistic tests on welded armor steel joints. *Metallography. Microstruct. Anal.* **2**, 125–139 (2013)
13. Sharma, V., Shahi, A.S.: Effect of groove design on mechanical and metallurgical properties of quenched and tempered low alloy abrasion resistant steel welded joints. *Mater. Des.* **53**, 727–736 (2014)
14. Kou, S.: *Welding Metallurgy*. Wiley, Hoboken (2003)
15. ASTM E384: Standard Test Method for Micro Indentation Hardness of Materials
16. ASTM E8: Standard Test Methods for Tension Testing of Metallic Materials
17. ASTM E23: Standard Test Methods for Notched Bar Impact Testing of Metallic